

AD-A133 731

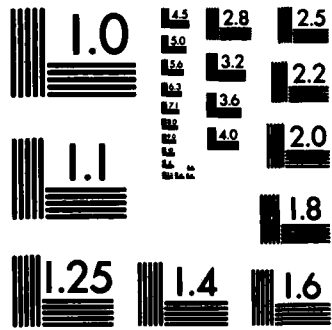
THE DETERMINATION OF MATERIAL PROPERTIES OF THE SEA BED
FROM THE ACOUSTIC... (U) NAVAL UNDERWATER SYSTEMS CENTERR
NEW LONDON CT NEW LONDON LAB. . D J THOMSON 13 SEP 83
UNCLASSIFIED NUSC-TD-6961

1/1

F/G 8/10 NL



END
FILMED
SEP 83



MICROCOPY RESOLUTION TEST CHART
NATIONAL BUREAU OF STANDARDS-1963-A

2

AD-A133 731

The Determination of Material Properties of the Sea Bed From the Acoustic Plane Wave Reflection Response

A Paper Presented at the Acoustics And the Sea Bed Conference, Bath, United Kingdom, 6-8 April 1983

D. J. Thomson
Surface Ship Sonar Department

DTIC
ELECTE
OCT 17 1983
S B



Naval Underwater Systems Center
Newport, Rhode Island / New London, Connecticut

Approved for public release; distribution unlimited.

83 10 17 176

WILL WPT

Preface

This document was prepared under Project No. 633K15. The sponsoring activity was the Surface Ship Sonar Department (Code 33), Naval Underwater Systems Center. The research for this document was funded principally by the Defence Research Establishment Pacific, Victoria, British Columbia, Canada.

The Technical Reviewer for this document was Dr. F. R. DiNapoli (Code 33).

Reviewed and Approved: 13 September 1983



L. Freeman
Head, Surface Ship Sonar Department

Dr. D. J. Thomson is an exchange scientist from the Defence Research Establishment Pacific, FMO, Victoria, British Columbia, VOS 1B0, Canada. He is presently located at the Naval Underwater Systems Center, New London, Connecticut 06320.

REPORT DOCUMENTATION PAGE		READ INSTRUCTIONS BEFORE COMPLETING FORM
1. REPORT NUMBER TD 6961	2. GOVT ACCESSION NO. AD-A133731	3. RECIPIENT'S CATALOG NUMBER
4. TITLE (and Subtitle) THE DETERMINATION OF MATERIAL PROPERTIES OF THE SEA BED FROM THE ACOUSTIC PLANE-WAVE REFLECTION RESPONSE	5. TYPE OF REPORT & PERIOD COVERED	
	6. PERFORMING ORG. REPORT NUMBER	
7. AUTHOR(s) Dr. David J. Thomson* *Exchange scientist from Defence Research Establishment Pacific, Victoria, B.C., Canada	8. CONTRACT OR GRANT NUMBER(s)	
9. PERFORMING ORGANIZATION NAME AND ADDRESS Naval Underwater Systems Center New London Laboratory New London, CT 06320	10. PROGRAM ELEMENT, PROJECT, TASK AREA & WORK UNIT NUMBERS 633K15	
11. CONTROLLING OFFICE NAME AND ADDRESS Naval Underwater Systems Center New London Laboratory New London, CT 06320	12. REPORT DATE 13 September 1983	
	13. NUMBER OF PAGES 10	
14. MONITORING AGENCY NAME & ADDRESS (if different from Controlling Office)	15. SECURITY CLASS. (of this report) UNCLASSIFIED	
	15a. DECLASSIFICATION / DOWNGRADING SCHEDULE	
16. DISTRIBUTION STATEMENT (of this Report) Approved for public release; distribution unlimited.		
17. DISTRIBUTION STATEMENT (of the abstract entered in Block 20, if different from Report)		
18. SUPPLEMENTARY NOTES		
19. KEY WORDS (Continue on reverse side if necessary and identify by block number) Acoustic plane wave Grazing angle Reflection coefficient Density profile Local wave Sea bed Forward scattering Inverse problem Sound speed profile Geoacoustic model Inversion algorithm		
20. ABSTRACT (Continue on reverse side if necessary and identify by block number) → Investigations of acoustic bottom reflectivity attempt to infer the structure of the sea bed (e.g., the density and sound speed profiles) from a limited knowledge of the reflection coefficient. For many applications, an adequate model to study the acoustic interaction is provided by the scattering of plane waves from a one-dimensional inhomogeneous medium. In contrast to formally exact solutions to this inverse scattering problem, Candel et al. (Journal of Sound and Vibration, vol. 68, 1980,		

20. (Cont'd)

pp. 571-595) propose an approximate scheme that can be readily implemented numerically. Their method applies the forward scattering approximation to a local wave decomposition of the acoustic field. As a result, the plane wave reflection coefficient is obtained as a nonlinear Fourier transform of the logarithmic derivative of the local admittance. Inversion of the integral transform enables the recovery of admittance versus depth by means of a numerical integration using a single impulse response from the sea bed. Separate recovery of both the density and sound speed profiles requires at least two impulse responses corresponding to two distinct grazing angles.

This paper appraises an implementation of Candel et al.'s inversion algorithm for the recovery of the density and sound speed profiles from two realistic geoacoustic models of the sea bed for which bandlimited impulse responses were synthetically generated.

Accession For	
NTIS GRA&I	<input checked="" type="checkbox"/>
DTIC TAB	<input type="checkbox"/>
Unannounced	<input type="checkbox"/>
Justification	
By	
Distribution/	
Availability Codes	
Dist	Avail and/or Special
A	

DTIC
COPY
INSPECTED
2

THE DETERMINATION OF MATERIAL PROPERTIES OF THE SEA BED FROM THE ACOUSTIC PLANE WAVE REFLECTION RESPONSE

INTRODUCTION

The detection capability of passive sonar systems that use bottom bounce propagation paths to estimate range and bearing to a target depends on the reflection coefficient of the sea bed. At low frequencies, the reflection process can be complicated by long wavelength sound waves that penetrate the surficial sediments. As a result, proper interpretation of the acoustic signals following subbottom interactions requires a knowledge of the material properties (e.g., the density and sound speed profiles) below the sea bed. A basic problem of underwater acoustics is how to accurately determine the structure of the sea bed from a limited knowledge of its reflection coefficient. For many applications, an adequate model to study this inverse problem is provided by the scattering of acoustic plane waves from a one-dimensional inhomogeneous medium.

Formal methods for solving the one-dimensional inverse scattering problem are reviewed by Burridge¹ and Newton.² In contrast to these exact solutions that provide few numerical results, Candel, DeFillipi, and Launay^{3,4} propose an approximate one that is readily implemented numerically. In their approach, the acoustic field is decomposed into the local upgoing and downgoing plane waves described in Claerbout.⁵ Application of the forward scattering approximation leads to an analytic representation for the reflection coefficient as a nonlinear Fourier transform of the logarithmic derivative of the local admittance. Inversion of the integral transform results in a numerical algorithm by which the admittance profile of the inhomogeneous medium can be recovered from integration of a single impulse response. At least two impulse responses corresponding to two distinct grazing angles of incidence are required to recover both density and sound speed profiles.

This paper reviews the basic results leading to the inversion algorithm of Candel et al.^{3,4} It also appraises the numerical implementation of their method for recovering both density and sound speed profiles from two realistic geoacoustic models of the sea bed for which impulse responses are synthetically generated.

BASIC THEORY

The mathematical model is shown in figure 1. The region $0 < z < H$ is occupied by an inhomogeneous liquid that has an arbitrary variation of density, $\rho(z)$, and sound speed, $c(z)$. The homogeneous regions are characterized by constant density, sound speed pairs: ρ_0, c_0 for $z < 0$ and ρ_1, c_1 for $z > H$. All regions are assumed to be nonabsorbing.

An acoustic plane wave, p_1 , initially propagating downward at an

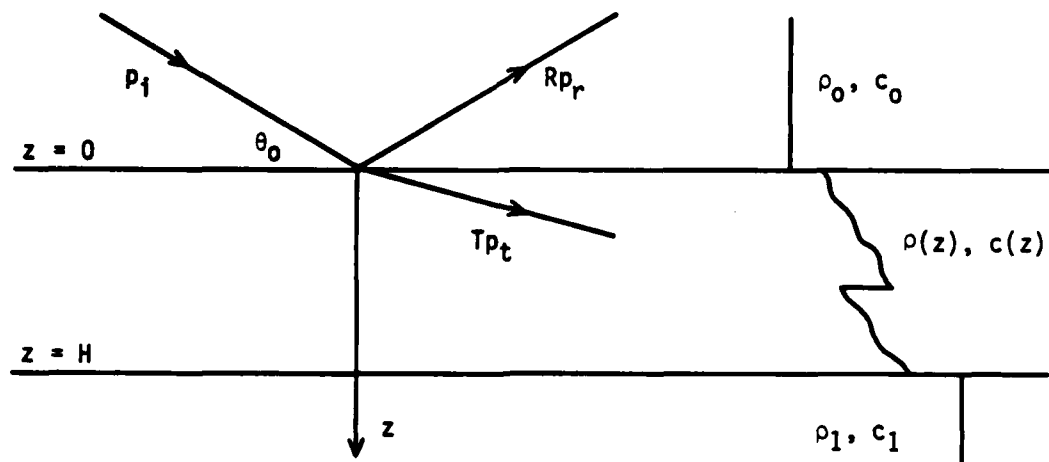


Figure 1. The Mathematical Model

angle, θ_0 , to the $z = 0$ plane encounters the inhomogeneous medium at $z = 0$. Within $0 < z < H$, the incident wave is partially reflected, and a reflected wave, $R P_r$, is returned to $z < 0$. In $z > H$, where no further reflections occur, only a transmitted wave, $T P_t$, continues to propagate.

For stratified media, all field quantities are independent of y (say) and exhibit a common wavenumber in the x -direction (i.e., $k_x = k_0 \cos \theta_0$). This number is fixed by the grazing angle of the incident wave. The assumption of time-harmonic waves with angular frequency, $\omega = 2\pi f$, allows suppression of the common factor, $\exp[ik_x x - i\omega t]$, from all field quantities.

The analytical route taken by Candel et al.^{3,4} to solve the one-dimensional inverse scattering problem is summarized in figure 2. In step (1), the plane wave reflection coefficient, R , is obtained formally by numerical integration of the basic equations, which are satisfied by the pressure, p , and the z -component of particle velocity, w . Here, Y_z is a "longitudinal admittance," defined as $Y_z = (k_z/k)/(\rho c) = k_z/(\omega \rho)$, where $k_z = [k^2 - k_x^2]^{1/2}$ is the z -component of the total wavenumber, $k = \omega/c$, at a given depth z . The splitting into a local upgoing wave, U , and a downgoing wave, D , shown in step (2), results in the local wave representation, shown in step (3). Although this splitting is not unique, as described by Schelkunoff⁵ and Sluijter,⁷ the local reflection coefficient, defined by $R = U/D$, gives the exact result for uniform media. For $|U| \ll |D|$, physical considerations suggest that the interpretation is suitable for inhomogeneous media. Application of the forward scattering approximation in step (4) results in an analytical representation for R as a nonlinear Fourier transform of the logarithmic derivative of the local admittance, g . For $|g| \ll 1$, this same result was obtained by Schelkunoff⁵ and Brekhovskikh.⁸ Transformation to the new depth coordinate, z^* , in step (5) results in a standard Fourier integral. Evaluation of the time response of R in step (6) determines the basic result that the impulse response at time, t , is related to the

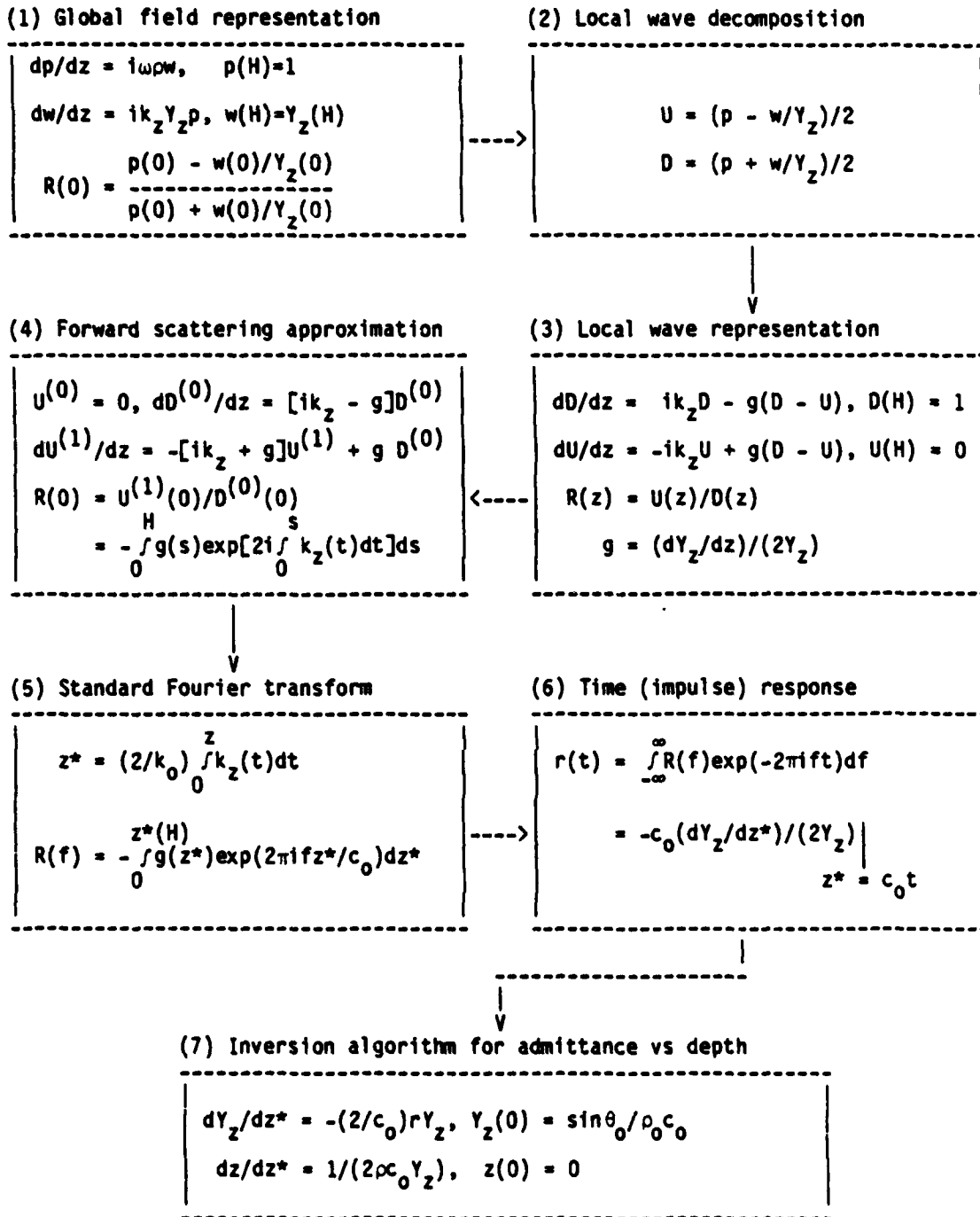


Figure 2. Flowchart of the Inversion Algorithm

variation in material properties about an "active" layer at depth, $z^* = c_0 t$. Finally, in step (7), two first order differential equations are obtained for the numerical determination of Y_z versus z from a single reflection sequence, $r(t)$.

Two aspects of this analysis deserve comment. First, the manipulations inherent in step (6) require that the relative variation of admittance be independent of frequency. Although this is a reasonable assumption for density and sound speed, usual treatments of absorption presume a linear dependence on frequency. For this reason, absorption was taken to be zero in the mathematical model. Second, although the forward scattering approximation leads to a direct, noniterative inversion algorithm, only primary reflections within the inhomogeneous medium can be accommodated. As a result, the presence of subbottom multiple reflections in the impulse response sequence can limit the depth to which the admittance profile can be recovered accurately.

The result in step (7) indicates that more information is required to recover both density and sound speed profiles. If the subscripts 1 and 2 are used to denote quantities corresponding to grazing angles θ_1 and θ_2 , where $\theta_2 > \theta_1$, then it can be shown that recovery of both ρ and $n = c_0/c$ can be obtained from the numerical integration of the four differential equations,

$$d(Y_z)_1/dz^*_1 = -(2/c_0) r_1 (Y_z)_1, \quad (1)$$

$$dz/dz^*_1 = [2\rho c_0 (Y_z)_1]^{-1}, \quad (2)$$

$$dz^*_2/dz^*_1 = (Y_z)_2/(Y_z)_1, \quad (3)$$

$$d(Y_z)_2/dz^*_1 = -(2/c_0) r_2 (Y_z)_2^2/(Y_z)_1, \quad (4)$$

together with the relations

$$\rho^2 c_0^2 = [\cos^2 \theta_1 - \cos^2 \theta_2]/[(Y_z)_2^2 - (Y_z)_1^2], \quad (5)$$

$$n^2 = [(Y_z)_2^2 \cos^2 \theta_1 - (Y_z)_1^2 \cos^2 \theta_2]/[(Y_z)_2^2 - (Y_z)_1^2]. \quad (6)$$

Equations (1) through (6) are the basis of the numerical results described in the remainder of this paper. Reflection responses are required for two probing directions, and four, instead of two, differential equations with appropriate initial conditions must be integrated.

GEOACOUSTIC MODELS

The density and sound speed profiles of the two geoacoustic models that provide the numerical simulations are shown in figure 3. Both geoacoustic

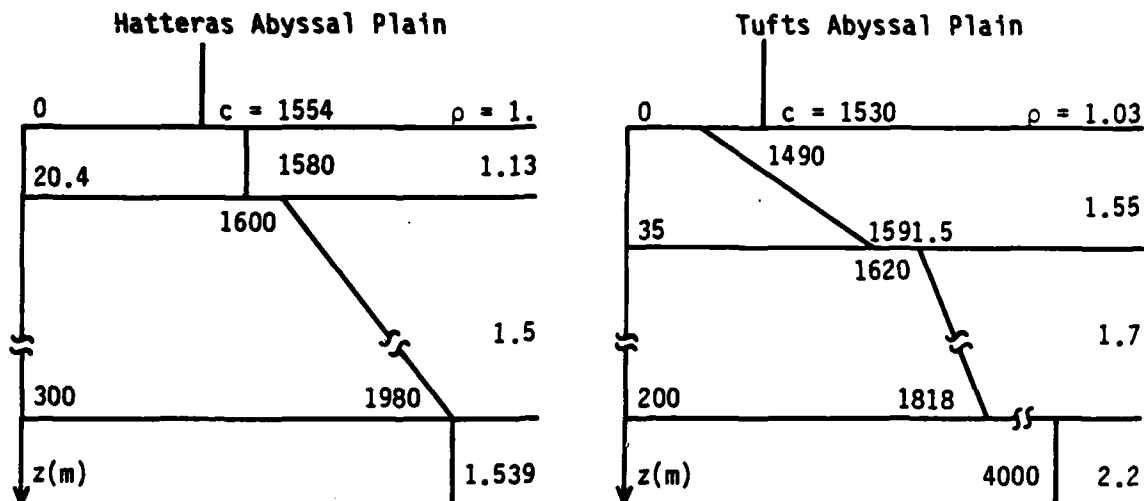


Figure 3. Profiles of Density, ρ (g/cm³), and Sound Speed, c (m/sec), as a Function of Depth, z (m), for the Geoacoustic Models

models were determined by analysis of deconvolved bottom reflected signals generated by explosive signal, underwater-sound (SUS) charges. The measurements for the Hatteras Abyssal Plain (28°30' N., 70°30' W.) were made by the Naval Underwater Systems Center (NUSC) and interpreted by Herstein, Dullea, and Santaniello.⁹ This model was used in other time-waveform simulations by DiNapoli, Potter, and Herstein.¹⁰ The measurements for the Tufts Abyssal Plain (46°00' N., 143°30' W.) were made by the Defence Research Establishment Pacific (DREP) and interpreted by Chapman.¹¹ Both models incorporate refracting sediment layers separated by discontinuities in material properties.

NUMERICAL RESULTS

The numerical examples provided by Candel et al.⁴ were restricted to waves propagating at normal incidence ($\theta_0 = 90^\circ$) in regions of constant density ($\rho = \rho_0$) only. For their results, recovery of $n(z)$ required only a single impulse response, as indicated in step (7) of figure 2. Thomson and Chow¹² extended the numerical implementation to include two impulse responses, corresponding to normal and oblique grazing angles, so that simultaneous recovery of both $\rho(z)$ and $n(z)$ is possible. For the geoacoustic models in figure 3, a similar approach is required.

For each geoacoustic model, the computer simulation proceeded as follows. At a given grazing angle, the complex, bandlimited frequency response, $R = \text{Re}[R] + i\text{Im}[R]$, was computed at 256 discrete frequencies, $f_k = k\Delta f$, $k = 0, 1, \dots, 255$, using $\Delta f = 0.5$ Hz. The sequence R was extended to $N = 1024$ points by appending zero values. A discrete fast Fourier transform was used to produce 1024 estimates of the time response, r , at $t_n = n\Delta t$, $n = 0, 1, \dots, 1023$, where $\Delta t = 1/(N\Delta f) = 1/512$ seconds. Each time response was convolved with a lowpass digital filter

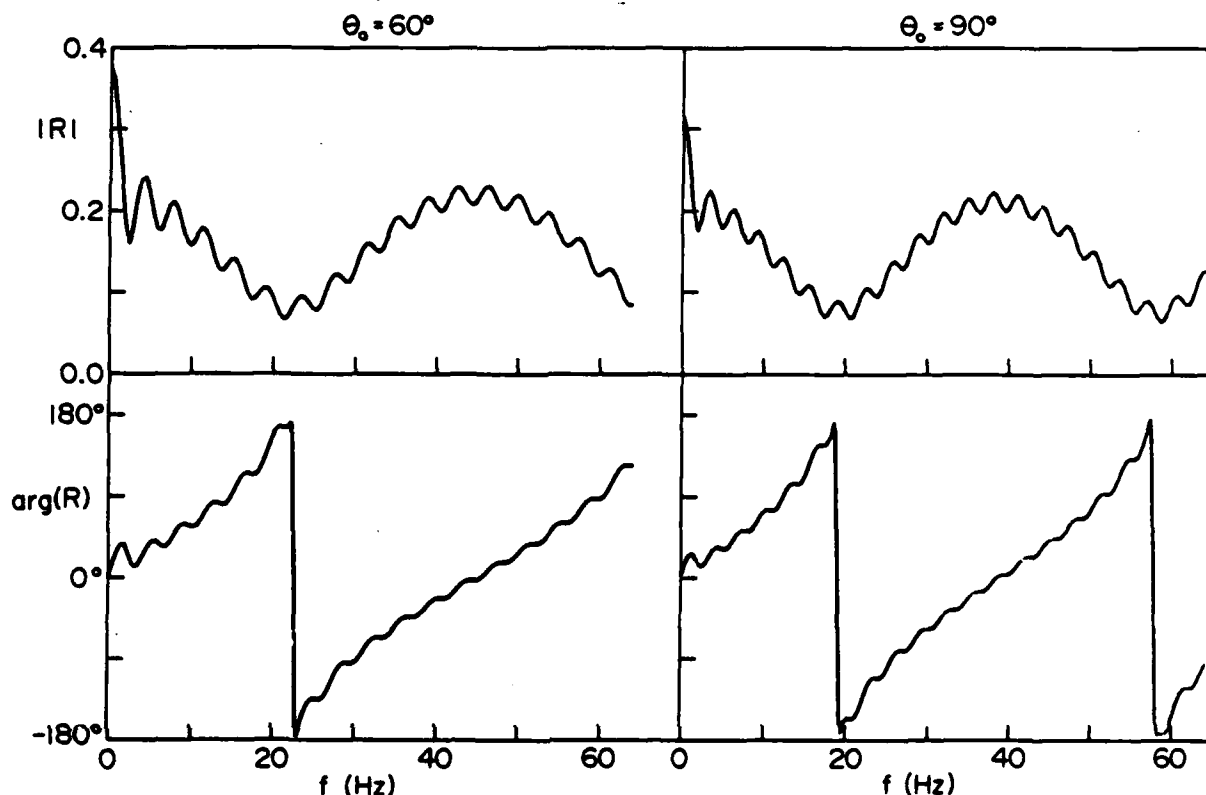


Figure 4. Frequency Responses of the Reflection Coefficient, $R = |R|\exp[i\arg(R)]$, at Grazing Angles of 60° and 90° for the Hatteras Abyssal Plain Model

designed using the window method as described by Kaiser and Reed.¹³ This filter inhibited Gibbs oscillations caused by sampling and truncation effects. For the results in this paper, a 31-point Kaiser window with a stopband suppression of 60 dB and a cutoff frequency of 64 Hz was used. Each filtered time response was multiplied by Δf to approximate the analytical Fourier transform result.

Figure 4 depicts the passband frequency responses of the reflection coefficient for the Hatteras Abyssal Plain model. The amplitude $|R|$, and phase, $\arg(R)$, are shown for grazing angles of 60° and 90° . $|R|$ exhibits two distinct modulations caused by reflections from layers of different thicknesses. $\arg(R)$ increases monotonically but is nonlinear because of the sound speed gradients within the thick layer. The greater amplitudes that occur for oblique incidence than for normal incidence are typical for impedance values that increase with depth.

The filtered impulse responses for this model are shown in the upper part of figure 5. The left trace corresponds to a grazing angle of 60° , and the right trace corresponds to a grazing angle of 90° . Each response is

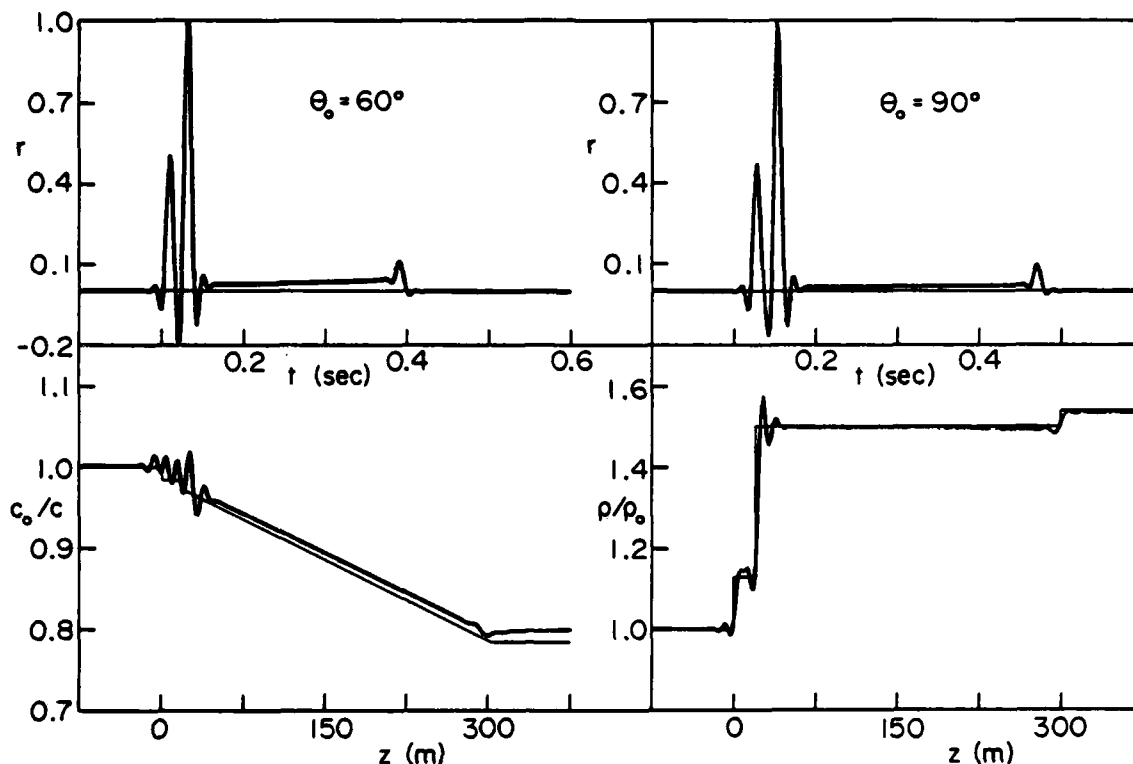


Figure 5. Filtered Time Responses of the Reflection Coefficients for Grazing Angles of 60° and 90° (Top) Used to Obtain the Normalized Density and Sound Speed Reconstructions for the Hatteras Abyssal Plain Model (Bottom)

normalized by its peak value. The initial time offset for each trace corresponds to the two-way travel time between $z = 0$ and a receiver located at $z = -100$ m. The smaller time offset observed for oblique incidence results from the plane wave propagating downward at the longitudinal phase speed, ω/k_z . The three "pulses" observed at both grazing angles are associated with discontinuities at the layer interfaces, $z = 0, 20.4$, and 300 m. Between the second and third reflections, continuous returns are observed, which are a result of the refracting nonzero sound speed gradients within the deep layer.

Use of these filtered time responses as input to equations (1) through (6) determines the reconstructed values of ρ/ρ_0 and $n = c_0/c$, shown in the lower part of figure 5. For comparison, the density and sound speed profiles of the Hatteras Abyssal Plain model used to generate the synthetic data are displayed on the same graphs. It is evident that the global behavior of the reconstructed profiles agrees with the model inputs. For the highest passband frequency used in the inversion process, the thin upper layer in this model is only 0.8 wavelengths thick. At this wavelength, the small changes in $n(z)$ are not resolved, although some of the difficulty is due to remanent Gibbs effects. It is interesting to note that the larger

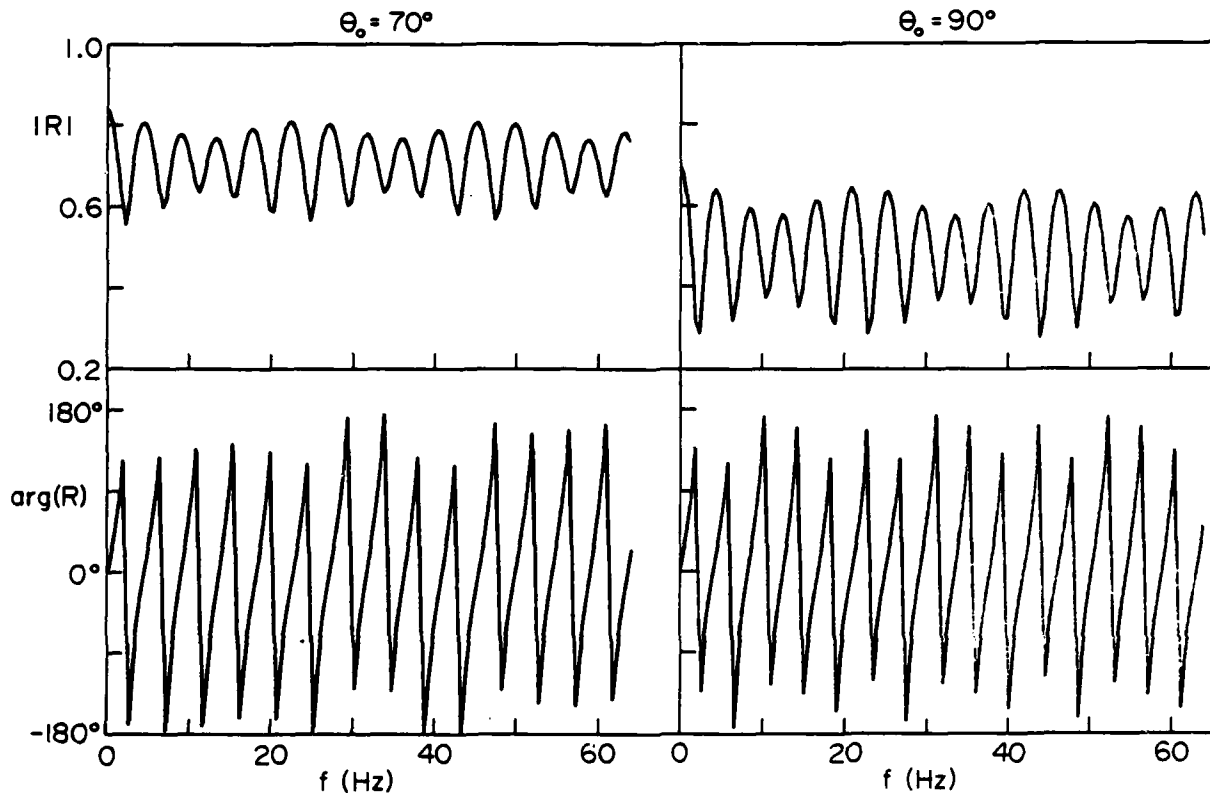


Figure 6. Frequency Responses of the Reflection Coefficient, $R = |R|\exp[i\arg(R)]$, at Grazing Angles of 70° and 90° for the Tufts Abyssal Plain Model

density variations within this layer are easily resolved by the bandlimited time responses.

Figure 6 shows the frequency responses of the reflection coefficients computed for the Tufts Abyssal Plain model. The large impedance increase at the base of the inhomogeneous region produces values of $|R|$ greater than those found for the Hatteras Abyssal Plain model. In this case, the forward scattering criterion, $|U| \ll |D|$, is only marginally satisfied. As before, a double modulation caused by interference between reflections at the top and bottom of each inhomogeneous layer occurs. The phase, $\arg(R)$, which changes rapidly with increases in frequency, is nonlinear because of the refracting sediments.

The filtered time responses, corresponding to the frequency responses given in figure 6, are presented in the upper part of figure 7. The first three "pulses" correspond to primary reflections from the interfaces, $z = 0$, 35, and 200 m. Multiple subbottom reflections arriving at later times are clearly visible. The lower part of figure 7 shows the reconstructed values of density and sound speed compared to the input values for the Tufts Abyssal Plain model. As in the previous example, the global agreement

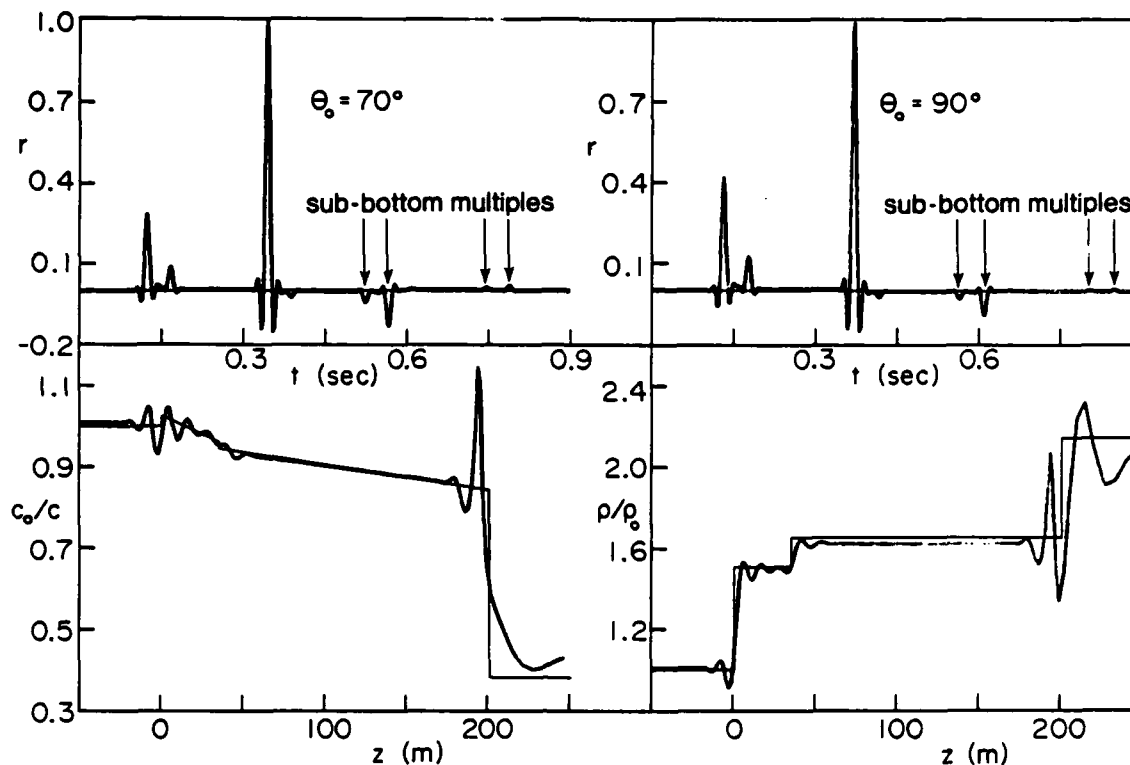


Figure 7. Filtered Time Responses of the Reflection Coefficients for Grazing Angles of 70° and 90° (Top) Used to Obtain the Normalized Density and Sound Speed Reconstructions for the Tufts Abyssal Plain Model (Bottom)

between reconstructed and model input profiles is excellent. Again, although $n(z)$ within the acoustically thin upper layer is not resolved by limitations of the 64 Hz band, the variations in density of this region are well defined. The local disagreement near $z = 200$ m apparently results from remanent Gibbs effects caused by imperfect filtering. For this model, reconstruction of the density and sound speed profiles to greater depths would be inappropriate because of multiple subbottom arrivals.

SUMMARY

This document has reviewed the direct inversion algorithm proposed by Candel et al.⁴ to recover the density and sound speed profiles of the sea bed from acoustic reflection data. A numerical implementation was applied to the reflection sequences generated synthetically for two representative geoaoustic models of deep water sediments. The reconstructed profiles showed excellent agreement with the model profiles even though the impulse responses were lowpass limited to 64 Hz. Although the results of the simulation are encouraging, two aspects of the inversion method require further study: (1) the effect of sediment absorption and (2) the effect of noise in the reflection data. This analysis is underway, and a report on the results is planned for the near future.

REFERENCES

1. R. Burridge, "The Gelfand-Levitan, the Marchenko, and the Gopinath-Sondhi Integral Equations of Inverse Scattering Theory, Regarded in the Context of Inverse Impulse-Response Problems," Wave Motion, vol. 2, 1980, pp. 305-323.
2. R. G. Newton, "Inversion of Reflection Data for Layered Media: A Review of Exact Methods," Geophysical Journal of the Royal Astronomical Society, vol. 65, 1981, pp. 191-215.
3. S. M. Candel, F. DeFillipi and A. Launay, "Determination of the Inhomogeneous Structure of a Medium From Its Plane Wave Reflection Response, Part I: A Numerical Analysis of the Direct Problem," Journal of Sound and Vibration, vol. 68, 1980, pp. 571-582.
4. S. M. Candel, F. DeFillipi and A. Launay, "Determination of the Inhomogeneous Structure of a Medium From Its Plane Wave Reflection Response, Part II: A Numerical Approximation," Journal of Sound and Vibration, vol. 68, 1980, pp. 583-595.
5. J. F. Claerbout, Fundamentals of Geophysical Data Processing, McGraw-Hill Book Company, Inc., New York, 1976.
6. S. A. Schelkunoff, "Remarks Concerning Wave Propagation in Stratified Media," Communications on Pure and Applied Mathematics, vol. 4, 1951, pp. 117-128.
7. F. W. Sluijter, "Arbitrariness of Dividing the Total Field in an Optically Inhomogeneous Medium Into Direct and Reversed Waves," Journal of the Optical Society of America, vol. 60, 1970, pp. 8-10.
8. L. M. Brekhovskikh, Waves in a Layered Media, Academic Press, New York, 1960.
9. P. D. Herstein, R. K. Dullea, and S. R. Santaniello, Hatteras Abyssal Plain Low Frequency Bottom Loss Measurements, NUSC Technical Report 5781, Naval Underwater Systems Center, New London, CT, 1979.
10. F. R. DiNapoli, D. Potter and P. Herstein, "Comparison of Synthetic and Experimental Bottom Interactive Waveforms," Bottom-Interacting Acoustics, Plenum, New York, NY, 1980.
11. N. R. Chapman, "Modeling Ocean Bottom Reflection Loss Measurements With the Plane Wave Reflection Coefficient," Journal of the Acoustical Society of America, vol. 73, 1983, pp. 1601-1607.
12. D. J. Thomson and R. K. Chow, Inversion of the Acoustic Plane-Wave Reflection Response of a Layered Ocean Bottom, NUSC Technical Report 6925, Naval Underwater Systems Center, New London, CT, 1983.
13. J. F. Kaiser and W. A. Reed, "Data Smoothing Using Low-Pass Digital Filters," Review of Scientific Instruments, vol. 48, 1977, pp. 1447-1457.

INITIAL DISTRIBUTION LIST

Addressee	No. of Copies
DARPA (TTO; Comdr. K. Evans)	2
CNO (OP-095; -098; Capt. E. Young, Comdr. H. Dantzler, 952D)	4
CNM (SPO PM-2; MAT-0723; Capt. E Harlett, -0724; R. Hillyer, -05; L. L. Hill, -907)	5
NAVELECSYSCOM (R. Mitnick, J. Schuster, 612; R. Knudsen, PME-124)	3
NAVSEASYSCOM (SEA-63R; D. Porter, F. Romano, R. Farwell, -63R)	4
NAVPGSCOL	1
DWTNSRDC	1
NORDA (R. Lauer, 320; S. Marshall, 115; R. Martin, 110A; E. Chiaka, B. Blumenthal, W. Worsley, R. Wheatly, 530; J. Matthews; G. Stanford; Library)	10
NOSC (M. Pederson, D. Gordon, 712; J. R. McCarthy, 713; C. Persons, 7133; S. Sullivan, 1604; R. Smith; J. Lovett; G. Tunstall; Library)	9
NAVAIRDEVCCEN (J. Howard; B. Steinberg; P. Haas; Library)	4
NCSC	1
NAVSURFWPNCEN (R. Stevenson; M. Stripling; M. Stallard; Library)	4
NRL (O. Diachok, R. Dicus, 5160; J. Munson, 5100; W. Mosley, 5120; A. Eller, 5109; Library)	6
MARINE PHYSICAL LAB, SCRIPPS (V. C. Anderson; F. Fischer; B. Williams)	3
NAVAIRSYSCOM (E. David, 370B; W. Parrigian, 370J)	2
NISC (H. Foxwell)	1
DTIC	2
ONR (R. Winokur, ONR-102B; Capt. E. Craig, T. Warfield, ONR-220; G. Hamilton, ONR-420; J. McKisic, ONR-4250A; P. Rogers, ONR-425UA; J. A. Smith; ONR-100; ONR-480)	9
DIA	1
CHESNAVFACENGCOM	1
ARL (University of Texas) (P. Vidmar; K. Hawker; R. Koch; Library)	4
ARL (Penn State University) (S. McDaniel; D. McCammon; Library)	3
Courant Institute (D. C. Stickler; Library)	2
Science Applications, Inc. (C. W. Spofford, R. Greene)	2
Cornell University (H. Schwetlick)	1
Northwestern University (G. Kriegsmann)	1
University of Denver (J. A. DeSanto, F. Hagin)	2
General Instrument Company (R. Breton)	1
FWG (P. Wille)	1
RSMAS (F. D. Tappert)	1

TD 6961

INITIAL DISTRIBUTION LIST (Cont'd)

Addressee	No. of Copies
CANADA	
DREP	20
DSIS (Microfiche Section, Report Collection)	3
DREA	1
ORAE Library (DMOR)	2
CDLS/L CDR	1
CDLS/W CDR	1
CMDO	1
DMRS	1
Commander Maritime Command (MC/ORD, SSO Ocean)	2
CFMMS	1
Maritime Headquarters Pacific (SSO Op Rsch)	1
DST(SE)3	1
DTA(M)3	1
RRMC (Dept. of Oceanography)	1
O Met Oc	1
Project Officer IEP ABCANZ-2, NOP 981, Pentagon	3
BRITAIN	
DRIC	3
AUWE	1
RAE	1
AUSTRALIA	
DRC	1
NEW ZEALAND	
DSE	1

END

FILMED

11-83

DTIC